Structural Characteristics of Thermotropic SmA Layer Phase Formed from Rigid-Rod Polysilanes

Hideki Oka, Goro Suzaki, Susumu Edo, Akiko Suzuki, Masatoshi Tokita, and Junji Watanabe*

Department of Organic and Polymeric Materials, Tokyo Institute of Technology, Ookayama, Meguro-ku, Tokyo 152-8552, Japan

Received July 16, 2008
Revised Manuscript Received September 22, 2008

The step-by-step development of liquid crystal (LC) order in rigid-rod polymers has been studied theoretically in the past two decades by using a computer simulation technique. In an early stage, Kimura et al.[1] gave the first indication that the smectic and columnar LC phases along with the nematic can be formed from aligned cylindrical molecules interacting through an excluded-volume effect. Subsequent simulation studies by Frenkel et al.[2,3] presented a complete phase diagram of perfectly aligned monodisperse spherocylinders as functions of the axial ratio of molecule and the molar density. It shows that the smectic A phase exists between the nematic phase with its lower density and the columnar phase with its higher density. Further, for a purpose of describing realistic liquid crystalline systems of synthetic polymers or biopolymers such as proteins, polysaccharides, and DNA, the phase behavior for molecules with polydisperse length have been investigated by Sluckin[4] and Bates and Frenkel.[5] The phase behavior in their calculations remained unchanged essentially from that observed in monodispersed system when the polydispersity is small. On increasing the polydispersity, however, the smectic phase becomes increasingly destabilized and finally disappears when it exceeds the critical value. Thus, the columnar phase is directly transformed to the nematic one in polydisperse systems.

Among the phases predicted in these theoretical approaches, the most interesting one is the smectic A (SmA) phase in which the rigid-rod polymers are packed laterally with their rod ends located at a limited space. Theoretical studies indicate that such a layer order can be achieved simply by the excluded volume effect; because of the effective accommodation of molecular ends, the packing density becomes larger than that in the nematic one. The layer spacing is speculated to be 1.2−1.3 times the molecular length.[1,3]

On the experimental side, lyotropic LC phases formed by rodlike helical biopolymers have been studied to clarify the step-by-step developing of LC structural ordering.[6−9] The smectic phase has been reported in the lyotropic system of synthetic polypeptide[10,11] and some viruses[12] with monodisperse molecular weight distribution, although the detailed studies on phase transition behavior have been interrupted because of difficulty in keeping volatile solvents within a vessel. In thermotropic systems, the SmA ordering was first speculated from the microscopic observation of fan-shaped texture and its characteristic flow behavior in the polypeptides.[13,14] Recently, the columnar−SmA−cholesteric phase sequence that precisely coincides with the theoretical prediction has been found in helical poly(γ-dodecyl L-glutamate)[15] and poly(*n*-decyl-2-methylbutylsilane) (PD2MBS)[16,17] with an exquisitely narrow molecular weight distribution. Among these two species of polymer, polysilane helix is idealistic to verify the above-mentioned theoretical results predicted only through the excluded volume interaction, since no significant electrostatic intermolecular attractions are included because of its nonpolar property.

In this communication, we report the structural characteristics of the SmA phase formed from poly[*n*-decyl-2-methylpropylsilane] (PD2MPS) with the following formula: PD2MPS assumes a helical conformation as the chiral PD2MBS homologue reported previously.[16] The rigid nature of polysilane backbone comes from the methyl branching in propyl side chain,[18,19] and the 7/3 helical conformation similar to the chiral PD2MBS polysilane[16] is formed as mentioned below. Left- and right-handed helical conformations are equally assumed since the molecule is not chiral. Thus, the cholesteric LC in the chiral PD2MBS polymer[16] is altered to the nematic one, leading to easy understanding of the phase transformation because of a lack of the cholesteric helical structure. PD2MPS were prepared with various molecular weights from 10 000 to 150 000. All these samples show the well-defined polymorphism with a sequence of columnar−SmA−nematic−isotropic. The detailed layer structure of SmA was analyzed by small-angle X-ray scattering and AFM methods.

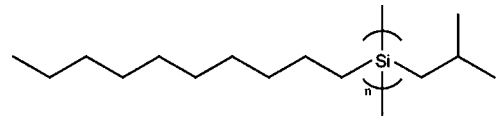

PD2MPS was synthesized with dichlorosilane monomer bearing 2-methylpropyl and *n*-decyl substituents by Wurtz-type condensation in toluene at 120 °C.[19] Since in this hard rod system the axial ratio of hard rod and polydispersity of its length are crucial to realize the smectic nature of LC phases, the synthesized polymers in toluene solution were fractionated by the fractional precipitation method with 2-propanol, ethanol, and methanol as precipitants. The nonpolar property of PD2MPS is advantageous to prepare the sample with sharp molecular weight distribution by this simple fractional precipitation method owing to the lack of aggregation in solution. Table 1 lists the molecular weights of resulting polymers, as determined by gel permeation chromatography (GPC) with a column of Shodex K-2004, using 40 °C chloroform as an eluent and with calibration by polystyrene standard. Fourteen samples were successfully prepared here with the molecular weights ranging from 13 700 to 151 000 and the polydispersities, M_w/M_n, from 1.07 to 1.39. The samples are coded here as PD2MPS-*X* where *X* indicates $M_w \times 10^{-3}$.

All the samples are like a milky wax at room temperature. The oriented X-ray diffraction pattern (the imaging plate by Rigaku RU200BH with Ni-filtered Cu Kα radiation) from this room temperature phase revealed several inner equatorial reflections with spacings of 1.70, 1.18, and 0.86 nm (see Figure S1). These reflections are assigned to orthogonal molecular packing with a two-dimensional lattice of $a = 1.70$ nm, $b = 2.36$ nm, and $\gamma = 90°$. As off-equatorial lines, two 0.44 and 0.34 nm lines showing *quasi*-meridional streaks and a 0.196 nm line with the meridional reflection can be recorded (Figure S1). These are attributed to the 7-residue 3-turn (7_3) helical conformation with a repeat length of 0.19 nm; the 0.44 and 0.34 nms lines are assigned to third and fourth layer lines, respectively, and the 0.196 nm meridional reflection to seventh

* Corresponding author. E-mail: jwatanab@polymer.titech.ac.jp.

10.1021/ma801606g CCC: $40.75
Published on Web 10/14/2008

Table 1. Molecular Weights, Transition Temperatures, and Smectic Layer Spacings of PD2MPS Polymers

			transition temperatures by microscopy observation									
			columnar	———	smectic A	———	nematic	———	isotropic	layer spacing/nm	
sample	M_w	M_w/M_n	T_1/°C		T_2/°C		T_i/°C[c]			SAXS	AFM
M-13.7	13 700	1.10	–[a]		109–111		120–140			12.9	
M-17.1	17 100	1.08	–		128–130		145–160			16.5	
M-20.0	20 000	1.08	–		142–146		160–170			18.5	
M-23.2	23 200	1.09	75 (75)[b]		154–156 (155)		176–186 (180)			20.5	16.7
M-26.2	26 200	1.11	–		163–169		185–195			22.4	18.4
M-32.1	32 100	1.07	(73)		177–179		186–200 (189)			26.6	
M-36.2	36 200	1.12	–		182–186		190–205			30.3	30.0
M-42.8	42 800	1.10	–		178–182		205–215				
M-57.6	57 600	1.16	(83)		171–177		215–235				50.2
M-75.7	75 700	1.15	(73)		187–193		190–220 (192)				
M-88.3	88 300	1.23	–		177–184		200–220				65.0
M-119	119 000	1.34	(72)		168–172		205–230				75.3
M-133	133 000	1.32	(73)		178–183		210–220				101.4
M-151	151 000	1.39	(74)		169–173		210–230				109.6

[a] Unclear. [b] DSC data in parentheses. [c] Transition temperatures higher than 200 °C are not reliable because the significant decomposition takes place.

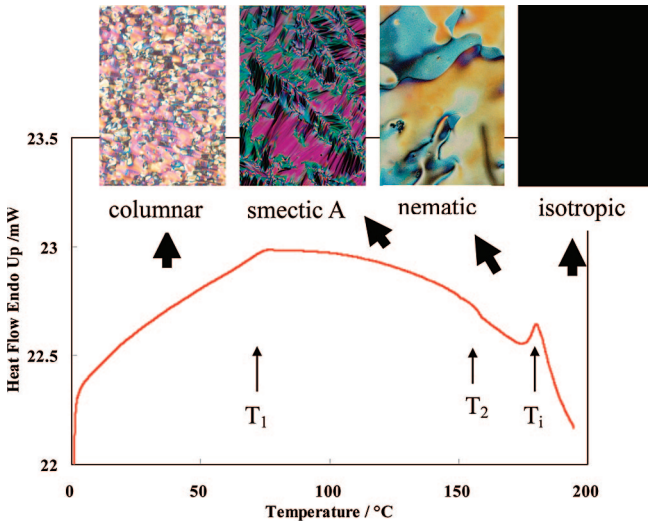

Figure 1. DSC thermograms of PD2MPS-23.2. Typical microscopic textures observed in respective temperature regions divided by the transitions at T_1, T_2, and T_i are shown in the inset.

layer line as observed in the chiral homologue.[16] No definite reflections on the layer lines show a random displacement of molecules along the chain axis. The density of around 1.0 g/cm^3 requires that two chains run through a unit cell. Two-dimensional positional order suggests a type of columnar LC phase (or some crystal phase).

On heating, the columnar phase transforms to the fluid birefringent phases and finally to the isotropic melt. Such a phase transition can be well detected by DSC thermogram as well as microscopic observation. A typical DSC thermogram observed for PD2MPS-23.2 is shown in Figure 1. Three transitions can be detected as broad but clear peaks: the first peat at T_1 = 75 °C (ΔH = ~0.1 kJ/mol), the second one at T_2 = 155 °C (ΔH = 0.03 kJ/mol), and the third one at T_i = 180 °C (ΔH = 0.3 kJ/mol). In microscopic observation, the mosaic-like texture at room temperature is altered to the fan-shaped texture at T_1 (see the microscopic textures in the inset of Figure 1). It then transforms to the schlieren texture at T_2 and finally the isotropic melt at T_i. Thus, optical microscopic data show the columnar–smectic–nematic–isotropic transition in order of increasing temperature. Transition temperatures collected from DSC and microscopic observations are listed in Table 1. For all the samples prepared here, the transition between the smectic and nematic phases and the isotropization of nematic phase were clearly determined from both methods, although the transition

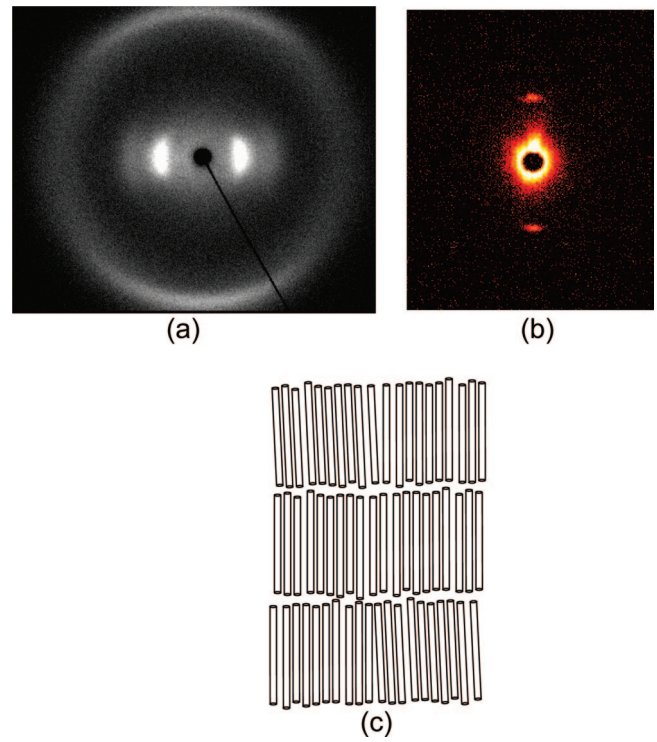

Figure 2. (a) WAXS and (b) SAXS patterns observed for the magnetically aligned SmA phase of PD2MPS-23.2 at 90 °C. The magnetic field was first applied for the nematic phase at 180 °C, and then the sample is cooled down to the smectic temperature of 90 °C at a rate of 5 °C/min. The field direction is vertical. In (c), the SmA structure of hard rod polysilane is illustrated.

between the columnar and smectic phases was sometime missed or spread widely. The T_2 and T_i temperatures increase on increasing M_w and then level off at around 40 000 (refer to Figure S2).

The orientation of the nematic phase is easily achieved by applying the magnetic field through the transformation from the isotropic phase. Its orientation is sustained in the following SmA and columnar phases on cooling. Parts a and b of Figure 2 show the wide-angle X-ray (WAX) and small-angle X-ray (SAX) patterns, respectively, taken for the oriented SmA phase of PD2MPS-23.2. Perfect orientation can be seen in both patterns. WAX pattern includes the broad reflection on equator which is perpendicular to the magnetic field. Its spacing of 1.45 nm corresponds to the lateral packing distance of polymers, meaning that the molecular long axes lie parallel to the magnetic field.

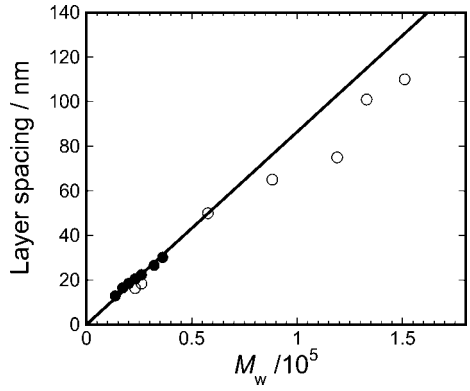

Figure 3. Molecular weight (M_w) dependence of SmA layer thickness. The closed and open circles were obtained from X-ray and AFM methods, respectively. The solid line indicates the length of polymers calculated as 0.196 nm times the degree of polymerization.

On the other hand, SAX pattern shows the clear reflection with a spacing of 20.5 nm on meridian. On transformation from SmA to nematic phase, this reflection disappears although a profile of the broad reflection in WAX pattern is not changed at all. Thus, it can be assigned to the smectic layer reflection. The layer spacing is not dependent on the temperature and nearly corresponds to the molecular length calculated with M_w and translational unit length per residue (0.196 nm), which identifies the SmA phase where the molecules lie perpendicular to the layer with their ends placed at a confined space as illustrated in Figure 2c. The smectic layer spacings are collected from the samples with molecular weights of 10 000−40 000 and plotted as closed circles against the molecular lengths calculated on the basis of M_w in Figure 3. The good correspondence between the observed spacings and the calculated molecular lengths can be found.

The small-angle X-ray method allows us to determine the layer spacings up to ∼40 nm. To collect the information on layer order with layer spacings larger than these values, AFM method was found to be the excellent way to detect the present layer structure. Typical examples of the AFM images are shown in Figure 4. Here, the films with thickness of ∼20 μm were cast on a glass plate from chloroform solutions, annealed for 1 h at smectic temperature, and then quenched to room temperature. AFM images were then taken with an Agilent Series 5500 atomic force microscope. Imaging was conducted in tapping mode using a silicon cantilever with a resonance frequency of 75 kHz. All of the AFM images show very clear topography characteristic to the layer repeating; this is because the density in a space between neighboring polymer layers is fairly lower than that of the polymer layer part. Their repeating lengths are plotted as open circles in Figure 3. In the region up to 40 nm, spacings from both X-ray and AFM methods well correspond to each other. In the region above 40 nm, the layer thickness determined by AFM method still increases proportionally, showing the persistent correspondence between the layer spacing and the molecular length up to the highest molecular weight sample of M_w = 151 000. Figure 5 shows the AFM layer topography in PD2MPS-133 observed over a wide area of 10 × 10 μm^2. The layer structure is found to be fairly ordered. No significant defects are contained except for a small number of edge dislocations. The spacing of adjacent layer (∼100 nm) remains constant throughout the whole region, i.e., over 100 layers. The correlation length along the layer is also long, which is beyond 10 μm.

In summery, we observed the well-defined thermotropic LC behavior with the columnar−SmA−nematic−isotropic phase

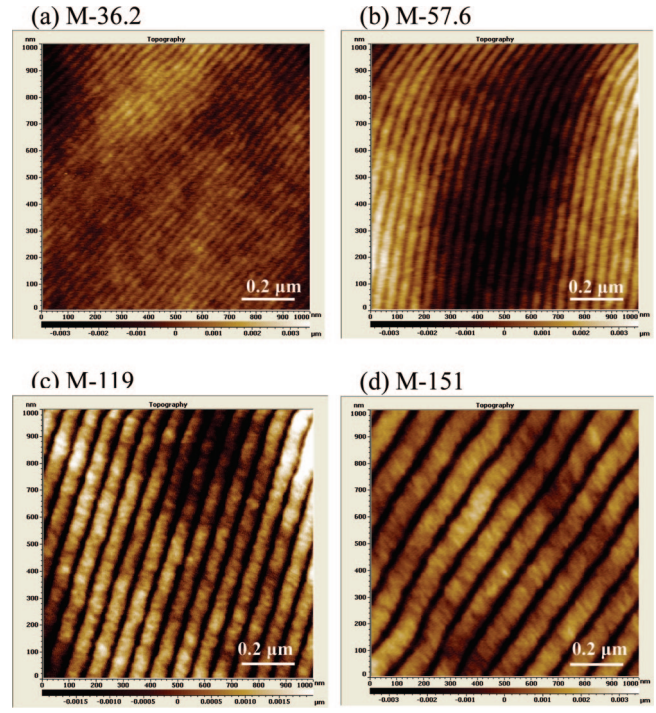

Figure 4. AFM image observed on the film surfaces of (a) PD2MPS-36.2, (b) PD2MPS-57.6, (c) PD2MPS-119, and (d) PD2MPS-151. The film samples with a thickness of ∼20 μm were cast on a glass plate from chloroform solutions, annealed at the SmA temperatures for 1 h, and then quenched to room temperature. All the samples show clear topography with a regular repetition of bright and dark parts which can be attributed to the smectic layer structure.

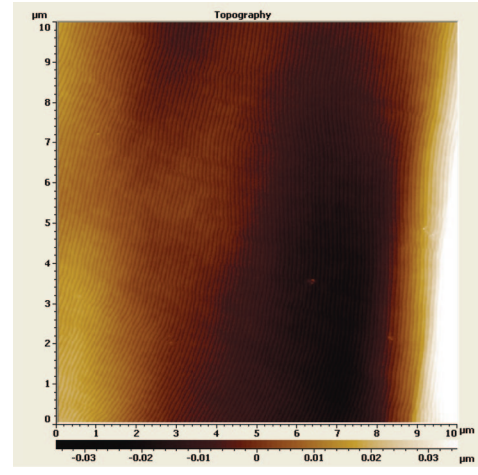

Figure 5. AFM image of the SmA layer structure observed over a wide area of 10 × 10 μm^2 in PD2MPS-133 film.

sequence in helical PD2MPS polysilanes with a wide variety of molecular weights of 13 700−151 000 and the narrow molecular weight distributions of 1.07−1.39. With respect to the notable SmA phase, AFM images illustrate the fantastic layer structure in which the spacing of adjacent layers remains constant throughout the whole region without significant defects, and the correlation length along the layer is fairly long beyond 10 μm. Such a long correlation length may be attributed to the high bent and splay elasticities in hard-rod polymer systems.[20] The layer thickness is varied from 10 to 110 nm depending on the molecular length, i.e., the molecular weight. Most striking in this study is the fact that the layer structure is regularly formed from the polymers with molecular weights as large as 150 000 irrespective of very small number density of polymer ends. Such

a consistent formation of the smectic layer structure with layer spacings comparable to the molecular lengths gives the opportunity to produce large-area nanostructures at easy processing which could be applied to developing optical and electronic devices.[21−23]

Acknowledgment. This research was supported by the Grant-in-Aid for Creative Scientific Research from Ministry of Education, Science, Sports and Culture in Japan.

Supporting Information Available: Figure S1 showing the X-ray patterns of oriented PD2MPS-23.2 and Figure S2 showing the molecular weight dependence of transition temperatures. This material is available free of charge via the Internet at http://pubs.acs.org.

References and Notes

(1) Hoshino, M.; Nakano, H.; Kimura, H. *J. Phys. Soc. Jpn.* **1982**, *51*, 741–748.
(2) Frenkel, D.; Lekkerkerker, H. N. W.; Stroobants, A. *Nature (London)* **1988**, *332*, 822–823.
(3) Bolhuis, P. G.; Frenkel, D. *J. Chem. Phys.* **1997**, *106*, 666–687.
(4) Sluckin, T. J. *Liq. Cryst.* **1989**, *6*, 111–131.
(5) Bates, M. A.; Frenkel, D. *J. Chem. Phys.* **1998**, *109*, 6193–6199.
(6) Livolant, F.; Bouligand, Y. *J. Phys. (Paris)* **1986**, *47*, 1813–1827.
(7) Livolant, F.; Levelut, A. M.; Doucet, J.; Benoit, J. P. *Nature (London)* **1989**, *339*, 724–726.
(8) Strzelecka, T. E.; Davidson, M. W.; Rill, R. L. *Nature (London)* **1998**, *331*, 457–460.
(9) Yen, C.-C.; Edo, S.; Oka, H.; Tokita, M.; Watanabe, J. *Macromolecules* **2008**, *41*, 3727–3733.
(10) Yu, S. M.; Conticello, V. P.; Zhang, G.; Kayser, C.; Fournier, M. J.; Mason, T. L.; Tirrell, D. A. *Nature (London)* **1997**, *389*, 167–170.
(11) He, S.-J.; Lee, C.; Gidio, S. P.; Yu, S. M.; Tirrell, D. A. *Macromolecules* **1998**, *31*, 9387–9389.
(12) Wen, X.; Meyer, R. B.; Caspar, D. L. D. *Phys. Rev. Lett.* **1989**, *63*, 2760–2763.
(13) Watanabe, J.; Takashina, Y. *Polym. J. (Tokyo)* **1992**, *24*, 709.
(14) In *Ordering in Macromolecular Systems*; Teramoto, A., Kobayashi, M., Norisue, T., Eds.; Springer: Berlin, 1993; p 99.
(15) Okoshi, K.; Sano, N.; Suzaki, G.; Tokita, M.; Magoshi, J.; Watanabe, J. *Jpn. J. Appl. Phys.* **2002**, *41*, L720−L722.
(16) Okoshi, K.; Kamee, H.; Suzaki, G.; Tokita, M.; Fujiki, M.; Watanabe, J. *Macromolecules* **2002**, *35*, 4556–4559.
(17) Okoshi, K.; Saxena, A.; Naito, M.; Fujiki, M.; Suzuki, G.; Tokita, M.; Watanabe, J. *Liq. Cryst.* **2004**, *31*, 279–283.
(18) Fujiki, M. *J. Am. Chem. Soc.* **2000**, *122*, 3336–3343.
(19) Naito, M.; Saeki, N.; Fujiki, M.; Ohira, A. *Macromolecules* **2007**, *40*, 648–652.
(20) In *Polymer Liquid Crystals*; Ciferri, A., Krigbaum, W. R., Meyer, R. B., Eds.; Academic Press: New York, 1982; Chapters 5 and 6.
(21) Guo, L. J. *J. Phys. D* **2004**, *37*, R123−R141.
(22) Lee, W.; Jin, M.-K.; Yoo, W.-C.; Lee, J.-K. *Langmuir* **2004**, *20*, 7665–7669.
(23) Zhang, C. Y.; Edo, S.; Ishige, R.; Tokita, M.; Watanabe, J. *Macromolecules* **2008**, *41*, 5361–5364.

MA801606G